



Article

A Comparative Study of the Electro-Assisted Grafting of Mono- and Bi-Phosphonic Acids on Nitinol

Bastien Arrotin ^{1,2}, Corentin Libiouille ¹, Tatiana Issakova ¹, Laetitia Mespouille ², Philippe Dubois ², Joseph Delhalle ¹ and Zineb Mekhalif ^{1,*}

¹ Laboratory of Chemistry and Electrochemistry of Surfaces (CES), University of Namur, rue de Bruxelles, 61, B-5000 Namur, Belgium; bastien.arrotin@unamur.be or bastien.arrotin@umons.ac.be (B.A.); corentin.libiouille@student.unamur.be (C.L.); tatiana.issakova@unamur.be (T.I.); joseph.delhalle@unamur.be (J.D.)

² Laboratory of Polymeric and Composite Materials (LPCM), Center of Innovation and Research in Materials & Polymers (CIRMAP), Health and Materials Research Institutes, University of Mons, Place du Parc, 23, B-7000 Mons, Belgium; laetitia.mespouille@umons.ac.be (L.M.); philippe.dubois@umons.ac.be (P.D.)

* Correspondence: zineb.mekhalif@unamur.be; Tel.: +32-(0)8172-5230; Fax: +32-(0)8172-4600

Received: 13 August 2019; Accepted: 25 September 2019; Published: 29 September 2019



Abstract: Over the last few years, Nitinol (NiTi) has become one of the most attractive alloy materials for industrial applications. However, its implementation is still problematic due to its surface nickel content, making it sensitive to pitting corrosion. In applications, it is often necessary to modify NiTi surfaces by using organic coatings, which provides new physico-chemical properties as well as functionalities and often contributes to a reinforcement of the alloy corrosion resistance. In this work, we assess the differences between the molecular layers made out of methylphosphonic acid (C₁P) and the bi-phosphonic acid derivatives: (methylimino)dimethylene-bisphosphonic acid (MIP₂) and 1-hydroxyethylidene-1,1-diphosphonic acid (HEP₂) using conventional (CG) and electro-assisted (EG) graftings. The surface modifications with the bi-phosphonic derivatives (MIP₂) and (HEP₂) carried out with the EG process lead to denser layers and a reinforced NiTi corrosion resistance.

Keywords: Nitinol; Electro-assisted grafting; mono- and bi-phosphonic acid derivatives; corrosion resistance

1. Introduction

Nitinol (NiTi), a nearly equiatomic nickel titanium alloy, is a major material for industrial applications [1–4]. It presents highly desirable intrinsic properties including heat, impact and corrosion resistance, high fatigue strength [1,5] super-elasticity, and shape memory [6–8]. As a consequence, NiTi is used in a wide range of applications such as self-expanding stents, surgical endoscopic instruments, atrial septal occlusion devices, orthodontic wires, orthopedic staples, and plates [9–14]. Its corrosion resistance results from the presence of a native TiO₂ passivating top-layer [15]. However, this very thin oxide layer still contains nickel inclusions, making it sensitive to pitting corrosion [16–18]. In recent years, various NiTi surface modification processes have been investigated, e.g., plasma treatment [19–21], chemical vapor deposition [22,23], hydrothermal reinforcement of the oxide layer [24,25], and the formation of organic self-assembled monolayers (SAMs) [26–28].

This last process is an attractive way to modify interfacial properties of NiTi, mainly by providing new physico-chemical surface properties such as wettability, protein adsorption resistance, biocompatibility, and/or bioactivity, and possibly reinforce their corrosion resistance. Among the various surface modifiers, organophosphonic acid derivatives robustly graft on metal oxide surfaces through hydrolysis resistant M-O-P bonds [29–33], thereby contributing to a strong reinforcement of the

metal surface against aggressive environments [32,34–37]. A common way to form such SAMs, referred to as conventional grafting (CG), is by direct immersion of the substrate in the organophosphonic solutions at different temperatures. An approach based on the anodic polarization of the substrate immersed in the organophosphonic solution, referred to in the sequel as electro-assisted grafting (EG), has been proposed recently by Mettoki et al. on Ti-6Al-4V [38]. Very recently, NiTi has been modified with organophosphonic derivatives by EG [39,40]. This approach has the advantage of leading to the formation of high quality SAMs within short modification times and at room temperature, which preserves temperature sensitive terminal functions of the organic surface modifiers [40].

Some molecules of interest present bulky terminal functions, which can lead to disordered and less protective layers. The use of mixed monolayers resulting from the co-adsorption of two organophosphonic acid derivatives differing in length and/or terminal functional groups has been shown to improve the corrosion resistance as well as the layer organization [41–44]. The present experimental work investigates the grafting on NiTi of short tail mono- and bi-phosphonic acid derivatives, which could be an alternative to the mixed monolayers approach, to find the most efficient anchoring group to be used in molecules of biological interests. For this purpose, surface modifications based on bi-phosphonic acid derivatives (*i.e.* (methylamino)dimethylene-bisphosphonic acid, MIP₂) and (1-hydroxyethylidene-1,1-diphosphonic acid, HEP₂) have been studied using both conventional (CG) and electro-assisted (EG) grafting approaches and compared to a mono-phosphonic acid derivative (methylphosphonic acid, C₁P) (Figure 1).

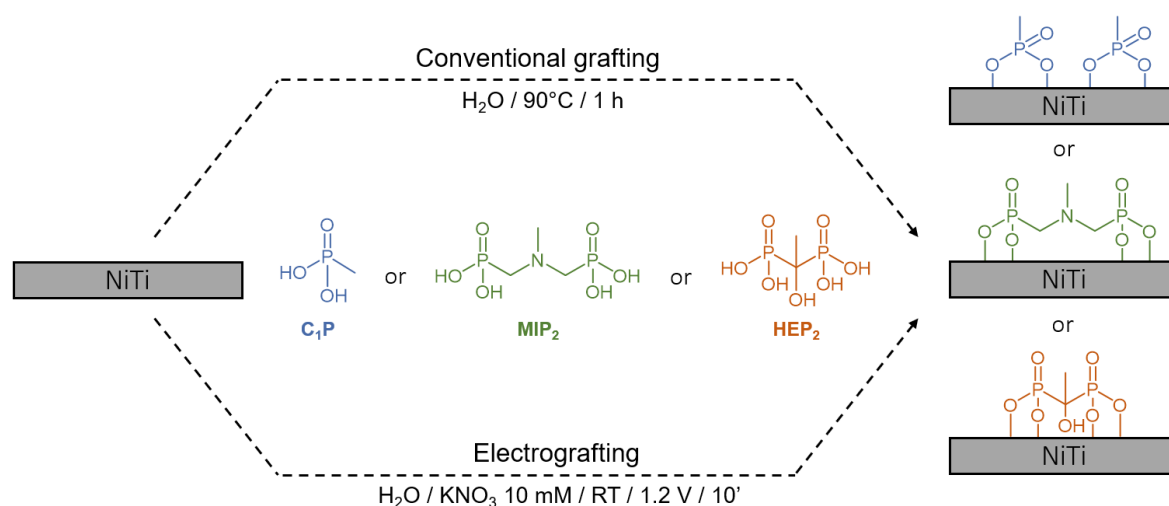


Figure 1. Schematic representation of the surface modification of Nitinol (NiTi) by conventional (CG) or electro-assisted (EG) grafting of phosphonic acid derivatives.

2. Experimental

2.1. Chemicals

Disolol®(ethanol 99% denatured with isopropanol 2% and butanone 2%, ChemLab, Zedelgem, Belgium), methylphosphonic acid (C₁P, 98%, Sigma-Aldrich, Overijse, Belgium), (methylamino)dimethylene-bisphosphonic acid (MIP₂, Specific Polymer, Castries; France), 1-hydroxyethylidene-1,1-diphosphonic acid (HEP₂, 95%, ABCR, Karlsruhe, Germany), potassium nitrate (98%, Overijse, Belgium), sodium hydroxide (98.5%, Acros Organics, Molinions, France) and sodium chloride (≥ 99.5%, Fluka, Hampton, United States) were used without further purification. All aqueous solutions were prepared in ultra-pure milli-Q water (18.2 MΩ cm).

2.2. Nitinol Substrates Preparation

Nitinol (Ni 56%/Ti 44%) rectangular-shaped plates (20 mm × 10 mm × 0.3 mm), purchased from AMF (Lury sur Arnon, France), were mechanically polished (Ecomet 300 instrument, Buehler, Esslingen, Germany) down to 0.1 μm roughness on silicon carbide papers using diamond pastes (9 μm) (Struers, Champigny sur Marne, France), a mixture of colloidal silica (MasterMet™ 2, Buehler, Esslingen, Germany) and H₂O₂ (35 wt.% solution in water, Acros Organics, Molinions, France).

Nitinol substrates were cleaned in denatured ethanol under ultrasonication for 15 min, blow dried with nitrogen, and stored under nitrogen for further use. Such samples are referred to here as Bare. Those samples submitted to a 1 h treatment in boiling water are called HT samples.

2.3. Conventional Grafting (CG) of the Organophosphonic Acid Derivatives on Nitinol

The chemical grafting (CG) on HT NiTi was achieved by its immersion (1 h at 90 °C) in 20 mL of 1 mM of the organophosphonic derivative (C₁P, MIP₂, or HEP₂) aqueous solution [40]. The substrates are then ultrasonically cleaned in denatured ethanol for 15 min before being blow dried under nitrogen.

2.4. Electro-Assisted Grafting (EG) of the Organophosphonic Acid Derivatives on Nitinol

Solutions (20.0 mL) composed of 1 mM of the organophosphonic derivative (C₁P, MIP₂ or HEP₂) and 10 mM KNO₃ are prepared in ultra-pure milli-Q water.

Electro-assisted grafting (EG) on the HT surface was obtained by immersion of the substrate in the solution for 10 min, under a voltage of 1.2 V vs. a saturated calomel electrode (SCE) [40] using a Princeton Applied Research VersaSTAT3 potentiostat/galvanostat. For comparison, a similar experiment (EG₀) has been carried out on the HT surface in absence of the organophosphonic derivatives. The substrates are then ultrasonically cleaned in denatured ethanol for 15 min, before being blow dried under nitrogen.

2.5. Substrate Characterization

The modified substrates are characterized by X-ray photoelectron spectroscopy (XPS), static water contact angle measurements (WCA), cyclic voltammetry (CV), linear sweep (LSV) voltammetry, electrochemical impedance spectroscopy (EIS), and roughness measurements. To assess the reproducibility of experiments, all analyses were performed in triplicate. In the case of XPS characterizations, each sample was also analyzed at three different locations.

XPS spectra were recorded on a K-Alpha spectrometer (Thermo Scientific, Waltham, United States) with a monochromatized X-ray K_α radiation (1486.6 eV), then the photoelectrons were collected at 0° with respect to the surface normal and detected with a hemispherical analyzer. The X-ray source spot size on the sample is 200 μm. The analyzer was operated with 200 eV and 50 eV as pass energy for the survey and the high-resolution core levels spectra, respectively. The core levels binding energy (BE) were calibrated with respect to the C1s BE set at 285.0 eV. Spectra were analyzed using a linear combination of Gaussian and Lorentzian curves in a 70/30 ratio. The peak areas were measured on core levels spectra. Quantitative XPS analyses were carried out by calculating the relevant abundance ratios on the basis of the core levels spectra and taking into account the corresponding Scofield sensitivity factors: [45] C1s 1.000, O1s 2.930, P2p 1.920, N1s 1.800, Ti2p 7.910 and Ni2p 22.180.

Static water contact angles were measured using a DIGIDROP (GBX Surface Technology, France) goniometer at room temperature and ambient atmosphere, with a syringe to deliver 2 μL milli-Q water droplets.

Electrochemical experiments were carried out on a Princeton Applied Research, Potentiostat/Galvanostat Model Versastat 3-LC using a three-electrode electrochemical cell with a controlled analysis spot surface (0.28 cm²). NiTi substrates, bare and modified, were used as a working electrode, a platinum foil as a counter electrode, and a saturated calomel electrode (SCE) as a

reference. Cyclic voltammograms were recorded from 0.10 to +0.65 V at a scan rate of 20 mV s⁻¹ in 0.1 M NaOH. The blocking factors (BF) of the coatings on NiTi were determined using the formula [46]:

$$BF = \frac{a_{an,0} - a_{an}}{a_{an,0}} \times 100 \quad (1)$$

where $a_{an,0}$ and a_{an} are the area of the anodic peaks for the first cycle of bare and modified NiTi substrates, respectively. The corrosion inhibition efficiency (IE) was determined from the corrosion current densities (j_{corr}) obtained by the formula: [46]

$$IE = \frac{j_{corr,0} - j_{corr}}{j_{corr,0}} \times 100 \quad (2)$$

where $j_{corr,0}$ and j_{corr} are the corrosion current densities of bare and modified NiTi substrates, respectively.

Linear sweep voltammograms were recorded from 0.2 V below OCP (measured for 1 h) to +1.0 V at a scan rate of 1 mV/s in 0.5 M NaCl.

EIS measurements are carried out in the frequency range of 10 kHz to 0.1 Hz at an amplitude of 10 mV peak to peak. The obtained EIS data were presented in Nyquist representation and were fitted to the electrical equivalent circuit shown in Figure 2, where R_{el} , R_{ct} and R_{layer} are the resistances of the electrolyte, of charge transfer, and of the surface layer (oxide layer or oxide/SAM layer), respectively, and where Q_{dl} and Q_{layer} are the constant phase element (CPE) of the electrochemical double layer and of the surface layer.

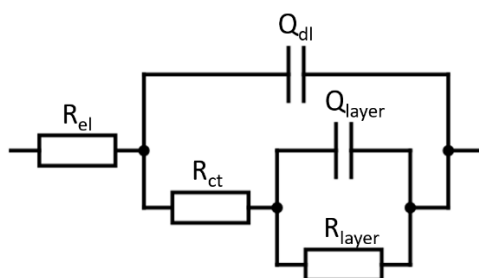


Figure 2. Electrical equivalent circuit used for the modeling of Nitinol.

The impedance of CPE, used to replace the capacitance element in non-ideal cases, is defined as [46]:

$$Z_{CPE} = \frac{1}{Q(j\omega)^n} \quad (3)$$

where Q is a frequency-independent parameter of the CPE. Deviation of the exponent n from ideal value $n = 1$ indicates the presence of inhomogeneity at the solid/electrolyte interface caused by roughness [47].

2.6. Molecular Modeling

The optimized molecular geometries of C_1P , HEP_2 , and MIP_2 were obtained by the molecular editor Avogadro using the molecular mechanics force field MMFF94.

3. Results and Discussion

The organophosphonic grafting through time-saving processes such as the electro-assisted approach was highly desirable either to activate the reaction and to improve the quality of the so-formed organic layer. This process is highly dependent on the number of partial charges carried by the molecule, thus influencing the way it will be attracted to the polarized electrode. For this purpose, the use of bi-phosphonic acid derivatives (MIP_2 and HEP_2) is compared to 1-methylphosphonic acid (C_1P).

Grafting of Organophosphonic Derivatives on HT Nitinol

C_1P , HIP_2 and MIP_2 were used to assess the grafting efficiency on the hydrothermally treated NiTi (HT) via the conventional (CG) and the electro-assisted (EG) processes with a particular attention on the anchoring group size impact on NiTi corrosion resistance. The footprint size, estimated from molecular modeling (Figure 3), of the mono-phosphonic C_1P and the bi-phosphonic derivatives, HIP_2 and MIP_2 , are 2.5, 5.6 or 7.3 Å, respectively. These molecules are grafted on HT NiTi plates by the conventional (CG) and electro-assisted (EG) procedures described in Sections 2.3 and 2.4, respectively.

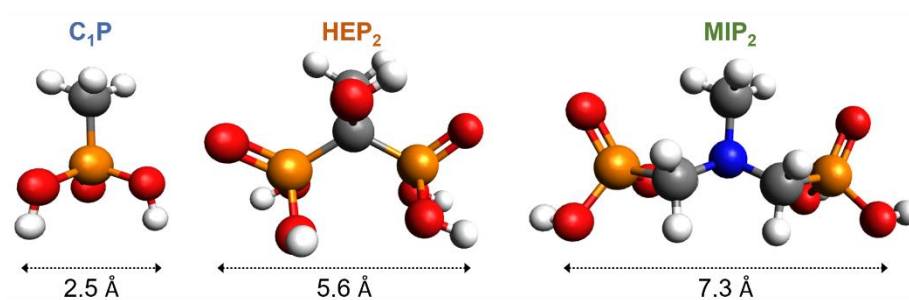


Figure 3. Simulated structured and estimated width of 1-methylphosphonic acid (C_1P), 1-hydroxyethylidene-1,1-diphosphonic acid (HEP_2), and (methylimino)dimethylene-bisphosphonic acid (MIP_2).

Figure 4 provides the water contact angle values. It is observed that, comparatively to HT and irrespective of the modification process (CG and EG), these values are slightly higher in the case of C_1P and MIP_2 and similar (or slightly smaller) for HEP_2 . This is consistent with the presence of the OH and of the CH_3 head group carried out by HEP_2 and by C_1P and MIP_2 , respectively (Figure 1). Moreover, the similar contact angle between the oxidized surface ($EG_0 - 22.2^\circ \pm 2.7^\circ$) and HEP_2 -covered NiTi ($22.2^\circ \pm 4.6^\circ$) can be explained by the presence of -OH group on HEP_2 and the potential hydroxylation of the oxide layer through EG_0 .

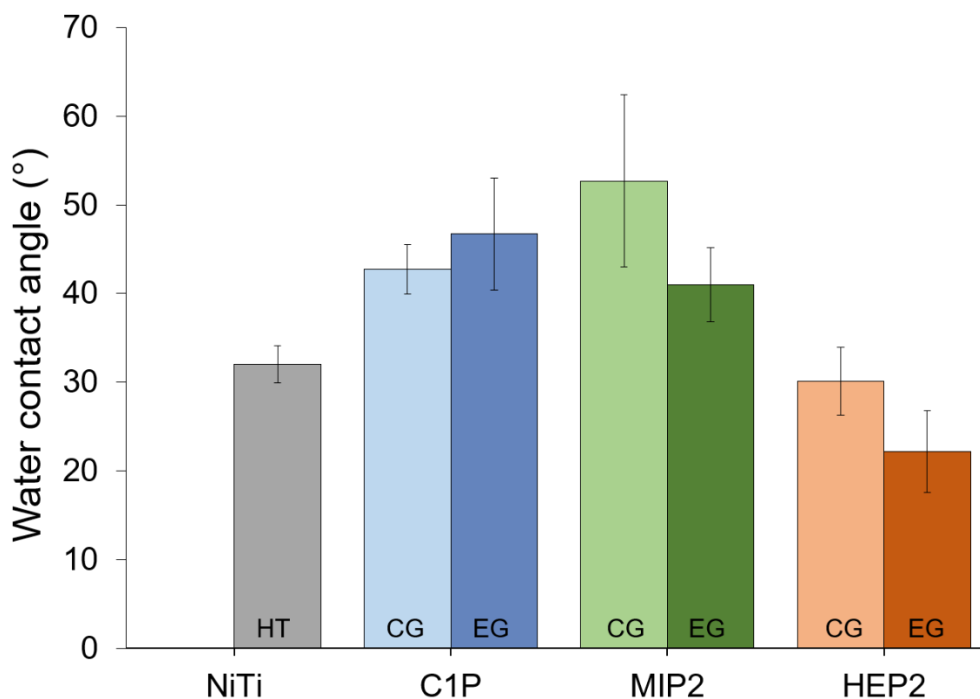


Figure 4. Water contact angles for hydrothermally treated NiTi (HT), C_1P , MIP_2 and HEP_2 .

XPS analyses performed on HT, C₁P, MIP₂, and HEP₂ confirm the successful modification of HT NiTi through the appearing signal of P2p and through the general shape of the obtained spectra for the C1s core level, as presented in Figure 5. These samples exhibit peaks at similar energies but with higher intensities in the case of modified NiTi with organophosphonic derivatives, indicating a successful organic modification of the surface alloy. The peaks at energies of 285, 286.5, 287.7, and 289.1 eV correspond respectively to carbon atoms involved in C-H/C-C, C-O/C-P/C-N, C=O, and O-C=O bonds present in the grafted molecules and contributions from atmospheric contaminations. The increase of the peak at 286.5 eV is particularly noticeable in the case of EG-MIP₂ and EG-HEP₂. XPS Ti2p and Ni2p core-levels for CG and EG, regardless of the type of grafted molecule, are consistent with the CG₀ and EG₀ results (Section 2.1), namely the metallic components of the Ti2p and Ni2p peaks are drastically reduced in the case of the EG treatment.

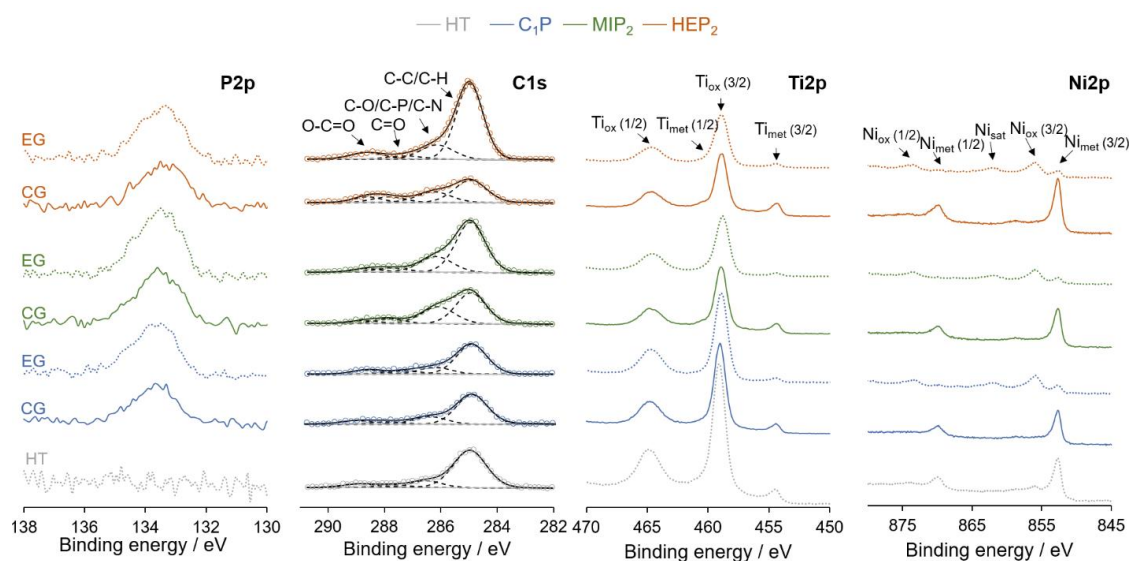


Figure 5. Representative X-ray photoelectron spectroscopy (XPS) core level spectra of P2p, C1s, Ti2p and Ni2p for HT NiTi, C₁P, MIP₂ and HEP₂.

The amount of NiTi is evaluated considering the total concentration of detected nickel and titanium (metallic and oxidized). The P/NiTi ratios are used to evaluate the amount of organic molecules grafted on the NiTi surface. The evolution of these ratios (Table 1) first attests to a better grafting efficiency (higher P/NiTi ratios) for the EG process. The presence of more phosphonic groups and thus more negative charges on the MIP₂ and HEP₂ molecules promotes their migration towards the anodically polarized sample.

Those results also attest for the formation of denser layers with bi-phosphonic than with mono-phosphonic molecules (Figure 6). For the modification with organophosphonic derivatives (Table 1), the Ni/NiTi ratios (0.13–0.15) are lower and O/NiTi (3.12–3.92) ratios are higher for EG comparatively to CG. Ni/NiTi ratios for the CG process are even higher (0.18–0.3) than for the HT treatment (0.15).

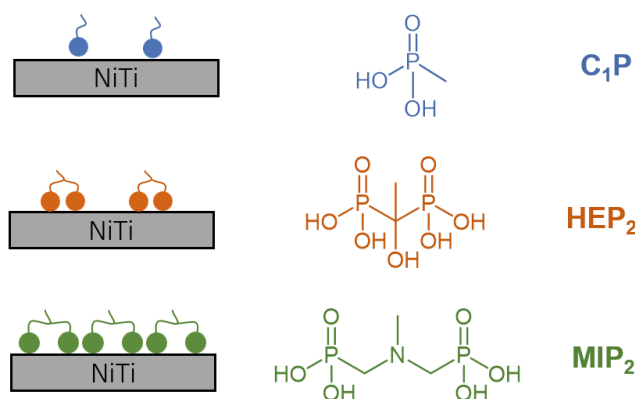


Figure 6. Schematic representation of the C₁P, HEP₂, and MIP₂ coatings obtained on HT NiTi.

Table 1. XPS atomic ratios for HT NiTi, C₁P, MIP₂, and HEP₂ samples.

Sample	P/NiTi	O/NiTi	Ni/NiTi	Ti/NiTi
HT	-	4.27 ± 0.70	0.15 ± 0.01	0.85 ± 0.01
C ₁ P (CG)	0.02 ± 0.01	2.65 ± 0.56	0.18 ± 0.04	0.82 ± 0.04
C ₁ P (EG)	0.05 ± 0.01	3.12 ± 0.21	0.13 ± 0.02	0.87 ± 0.02
MIP ₂ (CG)	0.09 ± 0.01	2.83 ± 0.23	0.21 ± 0.03	0.79 ± 0.03
MIP ₂ (EG)	0.14 ± 0.02	3.92 ± 0.36	0.15 ± 0.02	0.85 ± 0.02
HEP ₂ (CG)	0.08 ± 0.01	2.80 ± 0.23	0.30 ± 0.03	0.70 ± 0.03
HEP ₂ (EG)	0.12 ± 0.02	3.51 ± 0.90	0.15 ± 0.02	0.85 ± 0.02

The difference in the oxide layer composition between CG and EG processes and the nature of the grafting organophosphonic molecule have a synergetic effect and impact on NiTi corrosion resistance. Table 2 lists the corrosion current densities, the corrosion potentials, and the inhibition efficiencies for all NiTi treatments. In particular, it shows the superiority of C₁P and MIP₂ made by EG, which confer to HT-NiTi a very good corrosion protection highlighted by an inhibition efficiency of around 95%.

Table 2. Values of E_{corr} , j_{corr} , IE, BF and R_{layer} for HT NiTi, C₁P, MIP₂, and HEP₂ samples (obtained by LSV, CV, and EIS).

Sample	E_{corr} (mV vs. SCE)	j_{corr} (nA cm ⁻²)	IE (%)	BF (%)	R_{layer} (MΩ cm ⁻²)
HT	-284 ± 88	103.6 ± 22.2	-	-	2.900 ± 0.231
C ₁ P (CG)	-392 ± 20	8.5 ± 2.6	91.8 ± 2.5	12.5 ± 3.2	3.904 ± 0.514
C ₁ P (EG)	-189 ± 10	5.4 ± 1.6	94.8 ± 1.5	97.2 ± 0.5	10.562 ± 0.237
MIP ₂ (CG)	-463 ± 29	16.6 ± 2.6	83.9 ± 2.5	2.4 ± 0.4	3.149 ± 0.371
MIP ₂ (EG)	-371 ± 56	6.1 ± 2.4	94.1 ± 2.5	95.9 ± 2.9	9.247 ± 0.216
HEP ₂ (CG)	-354 ± 11	15.5 ± 2.6	85.1 ± 2.5	4.9 ± 1.1	3.576 ± 0.420
HEP ₂ (EG)	-182 ± 3	15.3 ± 0.9	94.9 ± 0.9	97.5 ± 0.5	10.934 ± 0.206

As attested to by the EIS measurements (Figure 7 and Table 2), this protection results from the increased surface layer resistance (R_{layer}) from 2.900 MΩ cm⁻² in the case of the HT-NiTi oxide layer to values of around 3 MΩ cm⁻² and 10 MΩ cm⁻² for C₁P, MIP₂, and HEP₂ made by CG and EG, respectively.

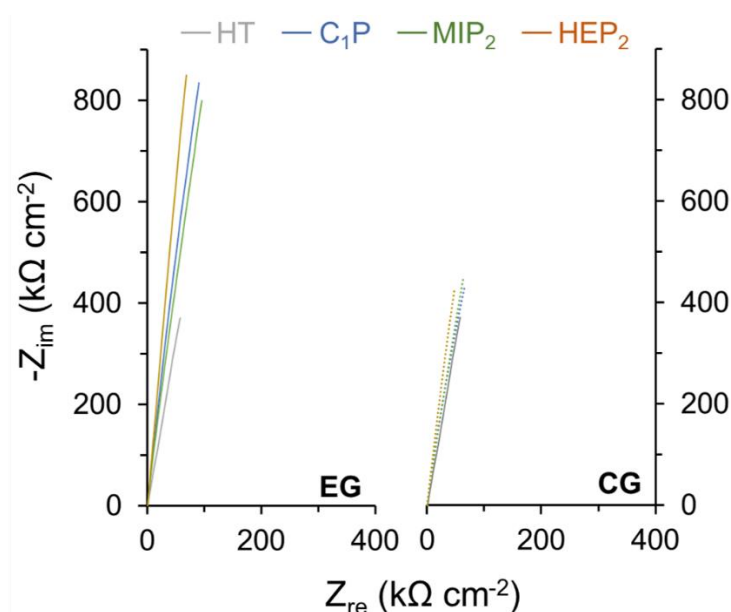


Figure 7. Representative electrochemical impedance spectra for HT NiTi, C₁P, MIP₂, and HEP₂ samples.

The alteration of the oxide layer within the CG process, which results in particular in an increase of Ni content (Table 1), is confirmed by CV measurements (Figure 8). The first CV cycles obtained for the CG-(C₁P, MIP₂, and HEP₂) show a larger oxidation peak, corresponding to a higher oxidation amount of Ti comparatively to HT-NiTi and the reappearance of the Ni²⁺ to Ni³⁺ oxidation peak, which is more detectable in the case of CG-(HEP₂). A higher blocking factor (BF) is obtained for EG up to 98.4%, resulting from a very low anodic current density and the absence of a nickel oxidation peak. CV, LSV and XPS results confirm the effectiveness of the electro-assisted grafting process (EG) regardless of the type of organophosphonic derivative.

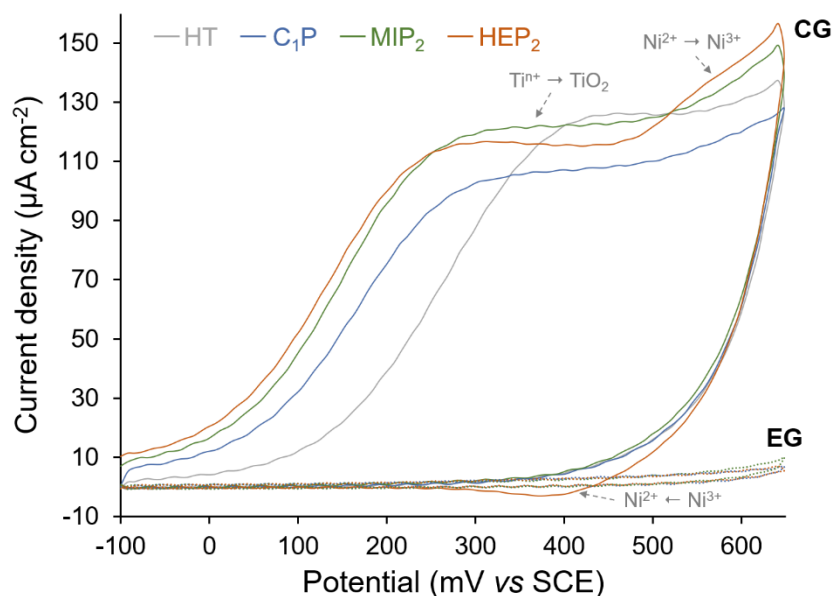


Figure 8. Representative first cycle of cyclic voltammograms for HT NiTi, C₁P, MIP₂, and HEP₂ samples in 0.1 M NaOH at a scan rate of 20 mV s⁻¹.

4. Conclusions

Nitinol alloy modified by conventional (CG) and electro-assisted (EG) grafting of three organophosphonic derivatives (C₁P, MIP₂, and HEP₂) with one or two anchoring groups has been compared.

The electro-assisted process, achieved in 10 min and at room temperature by anodic polarization of HT-NiTi has been shown to impact the oxide layer composition as well as the organophosphonic derivatives grafting reaction.

XPS results obtained for EG (C₁P, MIP₂, and HEP₂) point to a successful surface modification by C₁P, MIP₂, and HEP₂, as well as a reinforcement of the oxide layer. The use of molecules with larger footprint size increases the grafting rate and leads to the formation of denser layers, thanks to the presence of more partially negative charge on the molecules.

The impact of the nature of the molecule and the grafting process assessed by electrochemical techniques (LSV and CV) confirm the superiority of the EG process over the CG process. It leads to an enhancement of the corrosion resistance and to the formation of a more blocked surface. The EG process has two synergetic impacts: the reinforcement of the oxide layer and a high grafting efficiency of the organophosphonic derivatives. By contrast, the conventional grafting (CG) leads to a decreased corrosion resistance, with j_{corr} becoming up to three times higher and up to double the Ni surface content being obtained.

The (electro)grafting of bisphosphonic acid derivatives thus appear to be a promising alternative for mixed monolayers, which were previously used for the grafting of bulky polymerization initiators [44]. In this context, a monolayer made of a polymerization initiating specie deriving from HEP₂ or MIP₂ needs to be investigated.

Author Contributions: Conceptualization, Z.M.; Supervision, L.M., P.D. and J.D.; Writing—original draft, B.A. and T.I.; Writing—review & editing, C.L.

Acknowledgments: B.A., L.M. and P.D. acknowledge the Belgian Program on Interuniversity Attraction Poles initiated by the Belgian State, the Prime Minister's office (P7/05). CIRMAP is grateful to the "Belgian Federal Government Office Policy of Science (SSTC)" for general support in the frame of the PAI-7/05, the European Commission and the Wallonia Region (FEDER Program), and OPTI2MAT program of excellence. B.A. thanks UNamur and UMONS for the joint PhD grant.

Conflicts of Interest: The authors declare no conflict of interest.

References

1. Duerig, T.; Pelton, A.; Stöckel, D. An overview of nitinol medical applications. *Mater. Sci. Eng. A* **1999**, *273–275*, 149–160. [[CrossRef](#)]
2. Barras, C.D.J.; Myers, K.A. Nitinol—Its Use in Vascular Surgery and Other Applications. *Eur. J. Vasc. Endovasc. Surg.* **2000**, *19*, 564–569. [[CrossRef](#)]
3. Shabalovskaya, S.; Anderegg, J.; Van Humbeeck, J. Critical overview of Nitinol surfaces and their modifications for medical applications. *Acta Biomater.* **2008**, *4*, 447–467. [[CrossRef](#)] [[PubMed](#)]
4. Shayan, M.; Chun, Y. An overview of thin film nitinol endovascular devices. *Acta Biomater.* **2015**, *21*, 20–34. [[CrossRef](#)] [[PubMed](#)]
5. Elahinia, M.H.; Hashemi, M.; Tabesh, M.; Bhaduri, S.B. Manufacturing and processing of NiTi implants: A review. *Prog. Mater. Sci.* **2012**, *57*, 911–946. [[CrossRef](#)]
6. Centre d'Animation Régional en Matériaux Avancés (C.A.R.M.A.). *Alliages à Mémoire de Forme; Techniques de l'Ingénieur*: Saint-Denis, France, 2001.
7. Mantovani, D. Shape memory alloys: Properties and biomedical applications. *JOM* **2000**, *52*, 36–44. [[CrossRef](#)]
8. Mohd Jani, J.; Leary, M.; Subic, A.; Gibson, M.A. A review of shape memory alloy research, applications and opportunities. *Mater. Des.* **2014**, *56*, 1078–1113. [[CrossRef](#)]
9. Duerig, T.W.; Melton, K.N.; Stöckel, D. *Engineering Aspects of Shape Memory Alloys*; Butterworth-Heinemann: London, UK, 1990.

10. Airoidi, G.; Riva, G.; Vanelli, M. Superelasticity and Shape Memory Effect in NiTi Orthodontic Wires. *J. Phys. IV* **1995**, *5*, 1205–1210. [[CrossRef](#)]
11. Laster, Z.; MacBean, A.D.; Ayliffe, P.R.; Newlands, L.C. Fixation of a frontozygomatic fracture with a shape-memory staple. *Br. J. Oral Maxillofac. Surg.* **2001**, *39*, 324–325. [[CrossRef](#)] [[PubMed](#)]
12. Luebke, N.; Brantley, W.; Alapati, S.; Mitchell, J.; Lausten, L.; Daehn, G. Bending Fatigue Study of Nickel-Titanium Gates Glidden Drills. *J. Endod.* **2005**, *31*, 523–525. [[CrossRef](#)]
13. Nematollahi, M.; Baghbaderani, K.S.; Amerinatanzi, A. Application of NiTi in Assistive and Rehabilitation Devices: A Review. *Bioengineering* **2019**, *6*, 37. [[CrossRef](#)]
14. Eliaz, N. Corrosion of Metallic Biomaterials: A Review. *Materials* **2019**, *12*, 407. [[CrossRef](#)]
15. Shabalovskaya, S.A.; Rondelli, G.C.; Undisz, A.L.; Anderegg, J.W.; Burleigh, T.D.; Rettenmayr, M.E. The electrochemical characteristics of native Nitinol surfaces. *Biomaterials* **2009**, *30*, 3662–3671. [[CrossRef](#)]
16. Shabalovskaya, S.A.; Tian, H.; Anderegg, J.W.; Schryvers, D.U.; Carroll, W.U.; Van Humbeeck, J. The influence of surface oxides on the distribution and release of nickel from Nitinol wires. *Biomaterials* **2009**, *30*, 468–477. [[CrossRef](#)] [[PubMed](#)]
17. Figueira, N.; Silva, T.M.; Carmezim, M.J.; Fernandes, J.C.S. Corrosion behaviour of NiTi alloy. *Electrochim. Acta* **2009**, *54*, 921–926. [[CrossRef](#)]
18. Milošev, I.; Kapun, B. The corrosion resistance of Nitinol alloy in simulated physiological solutions Part 1: The effect of surface preparation. *Mater. Sci. Eng. C* **2012**, *32*, 1087–1096. [[CrossRef](#)]
19. Yang, J.; Wang, J.; Tong, S. Surface properties of bio-implant Nitinol modified by ECR cold plasma. *Mater. Sci. Technol.* **2004**, *20*, 1427–1431. [[CrossRef](#)]
20. Shen, Y.; Wang, G.; Chen, L.; Li, H.; Yu, P.; Bai, M.; Zhang, Q.; Lee, J.; Yu, Q. Investigation of surface endothelialization on biomedical nitinol (NiTi) alloy: Effects of surface micropatterning combined with plasma nanocoatings. *Acta Biomater.* **2009**, *5*, 3593–3604. [[CrossRef](#)]
21. Siu, H.T.; Man, H.C. Fabrication of bioactive titania coating on nitinol by plasma electrolytic oxidation. *Appl. Surf. Sci.* **2013**, *274*, 181–187. [[CrossRef](#)]
22. Lahann, J.; Klee, D.; Thelen, H.; Bienert, H.; Vorwerk, D.; Höcker, H. Improvement of haemocompatibility of metallic stents by polymer coating. *J. Mater. Sci. Mater. Med.* **1999**, *10*, 443–448. [[CrossRef](#)]
23. Catledge, S.A.; Thomas, V.; Vohra, Y.K. Effect of Surface Oxides and Intermetallics on Nanostructured Diamond Coating of Nitinol. *Curr. Nanosci.* **2006**, *2*, 9–12. [[CrossRef](#)]
24. Pérez, L.M.; Gracia-Villa, L.; Puértolas, J.A.; Arruebo, M.; Irusta, S.; Santamaría, J. Effect of Nitinol surface treatments on its physico-chemical properties. *J. Biomed. Mater. Res. B. Appl. Biomater.* **2009**, *91*, 337–347. [[CrossRef](#)]
25. Devillers, S.; Barthélémy, B.; Delhalle, J.; Mekhalif, Z. Induction Heating Vs Conventional Heating for the Hydrothermal Treatment of Nitinol and Its Subsequent 2-(Methacryloyloxy)ethyl 2-(trimethylammonio)ethyl Phosphate Coating by Surface-Initiated Atom Transfer Radical Polymerization. *ACS Appl. Mater. Interfaces* **2011**, *3*, 4059–4066. [[CrossRef](#)] [[PubMed](#)]
26. Quiñones, R.; Gawalt, E.S. Study of the formation of self-assembled monolayers on nitinol. *Langmuir* **2007**, *23*, 10123–10130. [[CrossRef](#)] [[PubMed](#)]
27. Petrovic, Z.; Katic, J.; Metikos-Hukovic, M.; Dadafarin, H.; Omanovic, S. Modification of a Nitinol Surface by Phosphonate Self-Assembled Monolayers. *J. Electrochem. Soc.* **2011**, *158*, F159–F165. [[CrossRef](#)]
28. Maho, A.; Kanoufi, F.; Combelle, C.; Delhalle, J.; Mekhalif, Z. Electrochemical Investigation of Nitinol/Tantalum Hybrid Surfaces Modified by Alkylphosphonic Self-Assembled Monolayers. *Electrochim. Acta* **2014**, *116*, 78–88. [[CrossRef](#)]
29. Marcinko, S.; Fadeev, A.Y. Hydrolytic Stability of Organic Monolayers Supported on TiO₂ and ZrO₂. *Langmuir* **2004**, *20*, 2270–2273. [[CrossRef](#)] [[PubMed](#)]
30. Bhure, R.; Mahapatro, A.; Bonner, C.; Abdel-Fattah, T.M. In vitro stability study of organophosphonic self assembled monolayers (SAMs) on cobalt chromium (Co–Cr) alloy. *Mater. Sci. Eng. C* **2013**, *33*, 2050–2058. [[CrossRef](#)] [[PubMed](#)]
31. Mahapatro, A.; Matos Negrón, T.D.; Nguyen, A. Spectroscopic Evaluations of Interfacial Oxidative Stability of Phosphonic Nanocoatings on Magnesium. *J. Spectrosc.* **2015**, *2015*, 350630. [[CrossRef](#)]
32. Guerrero, G.; Alauzun, J.G.; Granier, M.; Laurencin, D.; Mutin, P.H. Phosphonate coupling molecules for the control of surface/interface properties and the synthesis of nanomaterials. *Dalton Trans.* **2013**, *42*, 12569. [[CrossRef](#)] [[PubMed](#)]

33. Mani, G.; Johnson, D.M.; Marton, D.; Dougherty, V.L.; Feldman, M.D.; Patel, D.; Ayon, A.A.; Agrawal, C.M. Stability of Self-Assembled Monolayers on Titanium and Gold. *Langmuir* **2008**, *24*, 6774–6784. [[CrossRef](#)] [[PubMed](#)]
34. Ishizaki, T.; Okido, M.; Masuda, Y.; Saito, N.; Sakamoto, M. Corrosion resistant performances of alkanolic and phosphonic acids derived self-assembled monolayers on magnesium alloy AZ31 by Vapor-Phase Method. *Langmuir* **2011**, *27*, 6009–6017. [[CrossRef](#)] [[PubMed](#)]
35. Abohalkuma, T.; Telegdi, J. Corrosion protection of carbon steel by special phosphonic acid nano-layers. *Mater. Corros.* **2015**, *66*, 1382–1390. [[CrossRef](#)]
36. Quiñones, R.; Raman, A.; Gawalt, E.S. Functionalization of nickel oxide using alkylphosphonic acid self-assembled monolayers. *Thin Solid Films* **2008**, *516*, 8774–8781. [[CrossRef](#)]
37. Devillers, S.; Lemineur, J.F.; Dilimon, V.S.; Barthélémy, B.; Delhalle, J.; Mekhalif, Z. Polyelectrolyte multilayer deposition on nickel modified with self-assembled monolayers of organophosphonic acids for biomaterials: Electrochemical and spectroscopic evaluation. *J. Phys. Chem. C* **2012**, *116*, 19252–19261. [[CrossRef](#)]
38. Metoki, N.; Liu, L.; Beilis, E.; Eliaz, N.; Mandler, D. Preparation and characterization of alkylphosphonic acid self-assembled monolayers on titanium alloy by chemisorption and electrochemical deposition. *Langmuir* **2014**, *30*, 6791–6799. [[CrossRef](#)] [[PubMed](#)]
39. Vanhooland, A.; Devillers, S.; Issakova, T.; Michaux, C.; Delhalle, J.; Mekhalif, Z. Electroassisted Auto-Assembly of Alkylphosphonic Acids Monolayers on Nitinol. *J. Electrochem. Soc.* **2016**, *163*, G173–G177. [[CrossRef](#)]
40. Arrotin, B.; Delhalle, J.; Dubois, P.; Mespouille, L.; Mekhalif, Z. Electroassisted Functionalization of Nitinol Surface, a Powerful Strategy for Polymer Coating through Controlled Radical Surface Initiation. *Langmuir* **2017**, *33*, 2977–2985. [[CrossRef](#)]
41. Gupta, R.K.; Singh, R.A. Inhibition of corrosion by poly(N-hexadecylaniline)/docosanol mixed Langmuir–Blodgett films on copper in sea water. *Mater. Chem. Phys.* **2006**, *97*, 226–229. [[CrossRef](#)]
42. Li, C.; Li, L.; Wang, C. Study of the inhibitive effect of mixed self-assembled monolayers on copper with SECM. *Electrochim. Acta* **2014**, *115*, 531–536. [[CrossRef](#)]
43. Barthélémy, B.; Maheux, S.; Devillers, S.; Kanoufi, F.; Combellas, C.; Delhalle, J.; Mekhalif, Z. Synergistic Effect on Corrosion Resistance of Phynox Substrates Grafted with Surface-Initiated ATRP (Co)polymerization of 2-Methacryloyloxyethyl Phosphorylcholine (MPC) and 2-Hydroxyethyl Methacrylate (HEMA). *ACS Appl. Mater. Interfaces* **2014**, *6*, 10060–10071. [[CrossRef](#)] [[PubMed](#)]
44. Arrotin, B.; Noël, J.-M.; Delhalle, J.; Mespouille, L.; Mekhalif, Z. Electrografting of mixed organophosphonic monolayers for SI-ATRP of 2-methacryloyloxyethyl phosphorylcholine. *J. Coat. Technol. Res.* **2019**, *16*, 1121–1132. [[CrossRef](#)]
45. Chastain, J. (Ed.) *Handbook of X-ray Photoelectron Spectroscopy*; Perkin Elmer Corporation: Waltham, MA, USA, 1992.
46. Miomandre, F.; Sadki, S.; Audebert, P.; Méallet-Renaut, R. *Électrochimie: Des Concepts aux Applications*, 3rd ed.; Dunod: Malakoff, France, 2014.
47. Lukács, Z. Evaluation of model and dispersion parameters and their effects on the formation of constant-phase elements in equivalent circuits. *J. Electroanal. Chem.* **1999**, *464*, 68–75. [[CrossRef](#)]

